ISSN 1330-3651 (Print), ISSN 1848-6339 (Online)
UDC/UDK 624.014.2.075.23.042.8:519.6

NUMERICAL INVESTIGATION OF SEMI-RIGID COLUMN BASES WITH HYSTERESIS CHARACTERISTICS

Péter Iványi

Original scientific paper

The results of numerical experiments on dynamic response of a steel column, with a concentrated mass on the top are presented. The column is fixed in the base subjected to a triangular pulse force. Preisach hysteresis model was applied to investigate the dynamic behaviour of the steel column. In the solution of the non-linear dynamic equation of the motion the fix-point technique is inserted to the time marching iteration. The column base is modelled with a rotational spring of hysteresis characteristics. The top concentrated mass and the base rotation stiffness (hard, medium and soft hysteretic spring) were varied. The results are discussed based on the deflection (displacement) of the free end of the column in 10 s time period.

Keywords: *deflection, fix-point technique structural dynamics, non-linear dynamic equation, Preisach model, response*

Numeričko ispitivanje polu-krutih temelja stupova s karakteristikama histereze

Izvorni znanstveni članak

U radu se daju rezultati numeričkih eksperimenata dinamičke reakcije čeličnog stupa s masom koncentriranom na vrhu. Stup je učvršćen u temelju izloženom djelovanju trokutaste impulsne sile. Za ispitivanje dinamičkog ponašanja čeličnog stupa korišten je Preisachov model histereze. Za rješenje nelinearne dinamičke jednadžbe gibanja tehnika čvrste točke je umetnuta u vremensku iteraciju. Temelj stupa je medeliran s rotacionom oprugom s karakteristikama histereze. Masa koncentrirana na vrhu i rotaciona krutost temelja (tvrda, srednja i meka opruga histereze) su se mijenjale. Rezultati se razmatraju na osnovu progiba (pomaka) slobodnog kraja stupa u vremenskom razmaku od 10 s.

Ključne riječi: *progib, tehnika čvrste točke strukturalne dinamike, nelinearna dinamička jednadžba, Preisachov model, reakcija*

1 Introduction

In materials loaded by an impulse force a mechanical hysteresis loop is created when the strain varies between certain selected strain limits that remain in the plastic range. Several approaches have been introduced to describe the hysteretic behaviour of materials, for example the empirical kinetic approximation [1], the visco-plastic estimation [2], a one-parameter model [3] and the Ramberg-Osgood model [4 ÷ 5]. The Ramberg-Osgood model is a single values model, while the Preisach model allows multivalued characteristics. The Ramberg-Osgood model is compared to the Preisach model in [6]. Similarly the efficiency of the Jiles-Atherton and the Preisach models handling the non-linearity of magnetic materials has been shown [7 ÷ 9] and these methods have influenced the modelling of the non-linearity in mechanical systems as well [10].

In this paper the dynamic response of a steel column is determined from the non-linear equation of motion, which is combined with the Preisach hysteresis model. The structural dynamic system is excited by an impulse force and during the time marching iteration of the solution the fix-point technique is applied to the system of nonlinear equations.

2 Description of the model

In this paper a steel column is investigated with length l and a rectangular solid cross section of $a \times a$. The column has a fixed boundary condition at one end as it is shown in Fig. 1.

The mass of the steel column with an additional mass load is concentrated at the free end of the column and is denoted by m. A linearly increasing impulse force F is acting during time interval Δt on the free end of the structure. The column itself is considered as a completely rigid element, while the fixity condition at the end of the column is modeled by a rotational spring with a hysteresis property. The hysteresis property describes the relation between the bending moment and the declination angle of the column, which mean different boundary conditions for the column structure.

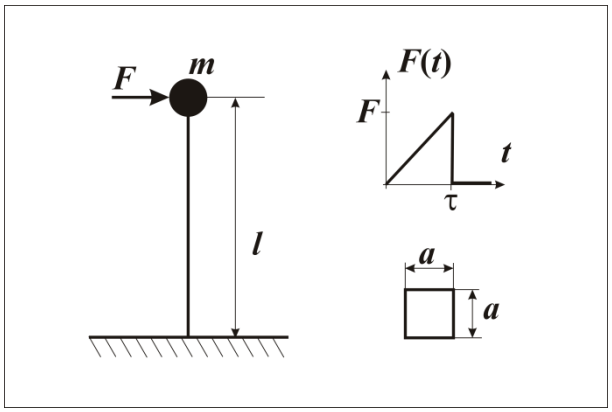

Figure 1 The arrangement of the steel structure, the cross-section of the column and the impulse loading condition

Combining the load of the external force F and the gravity effect of mass m at small displacement the acting force will be $f = F \cdot \cos\varphi + Q \cdot \sin\varphi$ (Fig. 2). The result of this combined load is a cyclic motion and a bending moment is generated at the column base. This paper investigates the relation between the deflection of the free end of the column and the generated bending moment of the spring at the column base when the characteristics of the rotational spring are modeled with a Preisach hysteresis model.

The equation of motion of the structure can be expressed as in [11, 12]:

$$m\ddot{x}(t)+c\dot{x}(t)+P(x)=f(t), \tag{1}$$

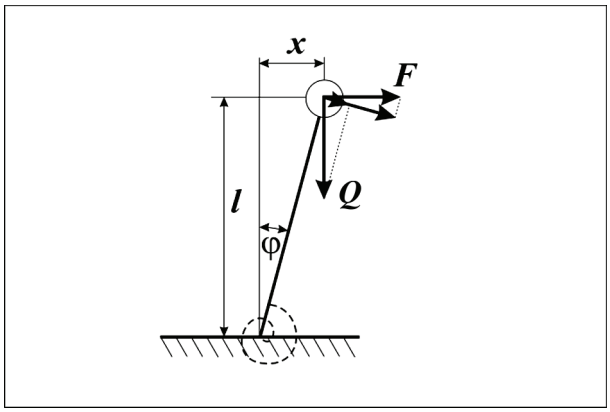

Figure 2 The mechanical model of the steel column including the force components (*F, Q*), the displacement (*x*), the declination angle (φ) and the rotational spring.

where m is the mass, c is the equivalent damping coefficient, $P(x)$ is the non-linear characteristics of the rotational spring and x is the deflection, which is assumed to be "small", therefore the small displacement theory holds true. The damping coefficient can be expressed as $c=\alpha/50\cdot\sqrt{k\cdot m}$, [13], where $\alpha(\%)$ is the system-damping coefficient and k is the stiffness parameter of the column, which can be calculated as $k=3\cdot E\cdot I/l^3$, where E is the Young modulus, I is the second moment of cross section ($I=a^4/12$). From deflection x generated by the external and the gravity force a bending moment, $M=\left(F\cdot\cos\varphi+Q\cdot\sin\varphi\right)\cdot l$ will act at the column base (Fig. 2), where φ is the declination angle and M is the bending moment. Considering small rotation, it is true that $\cos\varphi\approx 1$ and $\sin\varphi\approx\varphi\approx x/l$, and in Eq. 1 the acting force $f(t)$ is:

$$f(t)=F(t)+Q\cdot x(t)/l\,. \tag{2}$$

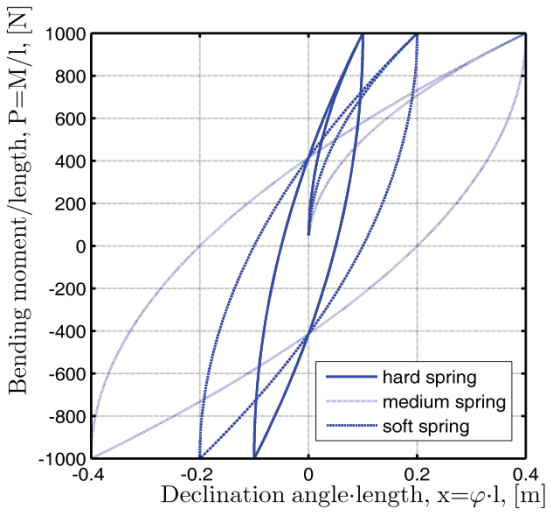

Figure 3a The direct hysteresis characteristics of rotational spring

For the hysteresis characteristics of the rotational spring the declination angle is converted to deflection $x=\varphi l$ with respect to the spring force $P=M/l$. In mechanical structures the 'direct' characteristics of the rotational spring $P=H\{x\}$ is applied, Fig. 3a, however in this case according to the Preisach hysteresis model the 'inverse' characteristic of the rotational spring is known as $x=H'\{P\}$ where deflection x is expressed with respect to the spring force P.

In this paper an investigation is performed where the rotational spring is modeled with soft, medium and hard characteristics, as it is shown in Fig. 3b.

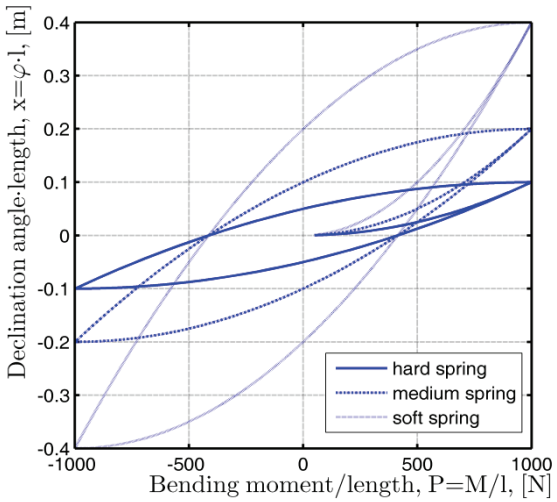

Figure 3b The inverse hysteresis characteristics of rotational spring: hard spring (solid line), medium spring (dashed line) and soft spring (dotted line)

3 The non-linear iteration

For the time solution of the dynamic problem of Eq. 1 the Crank-Nicholson schema is applied twice. The non-linear iteration is realized by the fix-point technique [14 ÷ 15] to have a contract transformation of the direct characteristics

$$P(x)=k_{FP}\cdot x+R\,, \tag{3}$$

where k_{FP} is the fix-point constant to represent the linear part of the approximation and R is the remaining non-linearity. Substituting Eq. (3) into Eq. (1) at a fixed time moment the resulting equation is:

$$m\ddot{x}^{i+1}+c\dot{x}^{i+1}+k_{FP}\cdot x^{i+1}=f^{i}-R^{i}\,, \tag{4}$$

where the superscript expresses the iteration step at any time moment and the iteration steps are the following:

Step 1.

At the new $n+1$ time step the initial value of the deflection is equal to the last value of the previous time step, $x^i=x^n$, the initial value of the non-linear part of the hysteresis is equal to the last value of the previous time step, $R^i=R^n$;

Step 2.

The value of force f^i is known with respect to deflection x^i as $f^i=F^{n+1}+Q\cdot x^i/l$;

Step 3.

By the solution of Eq. (4) a new iteration for x^{i+1} can be determined;

Step 4.

An estimation for the force of the rotational spring can be determined as $P^{i+1} \approx k_{FP} \cdot x^{i+1} + R^i$;

Step 5.

With the help of the hysteresis the remaining non-linear part can be calculated as
$R^{i+1} = P^{i+1} - k_{FP} \cdot H'\left\{P^{i+1}\right\}$;

Step 6.

The iteration continues on while
$\left\|R^{i+1} - R^i\right\| > \varepsilon \left\|R^{i+1}\right\|$, then
$x^i = x^{i+1}$, $R^i = R^{i+1}$ and go to Step 2.

Step 7.

When the iteration has converged, advance the time step and go to Step 1.

4 Numerical results and discussions

For the numerical investigation of the above described problem the following parameters have been selected for all numerical experiments: the length of the column is $l = 10$ m and the solid cross-section is $a \times a = 0{,}1 \times 0{,}1\,\mathrm{m}^2$. The time step is constant during all simulations: $\delta t = 0{,}05$ s .

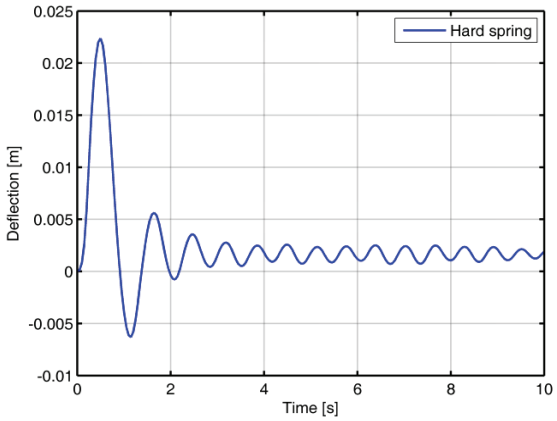

Figure 4a Deflection of the free end of the column under 1 kN external force when the rotational spring at the column base has hard characteristics (Test 1).

In the first four numerical experiments (Test 1-4) the system-damping (α) is zero, the mass at the top of the column is $m = 10^3$ kg and the external force will act during $\Delta t = 0{,}2$ s interval. In the case of Tests 1 and 2 the external force is $F = 1$ kN. These parameters and the spring characteristics are (hard and soft) shown in Tab. 1.

The deflection of the free end of the column is plotted in Fig. 4a for the rotational spring with hard characteristics and in Fig. 4b for the soft characteristics.

From the figures and Tab. 1 it can be seen that the soft rotational spring has larger deflection under the same external force and mass conditions. The time period of the dynamic vibration T_{osc} for the soft rotational spring is longer than for the hard rotational spring.

Table 1 Parameters and results of the numerical experiments Test 1-4

Test	F / kN	Spring	T_{osc} / s	$x_{\max}$ / m	$t_{\max}$ / s
1	1	hard	0,65	0,0224	0,50
2	1	soft	1,25	0,0408	0,75
3	2	hard		0,0582	0,60
4	2	soft		0,1063	0,90

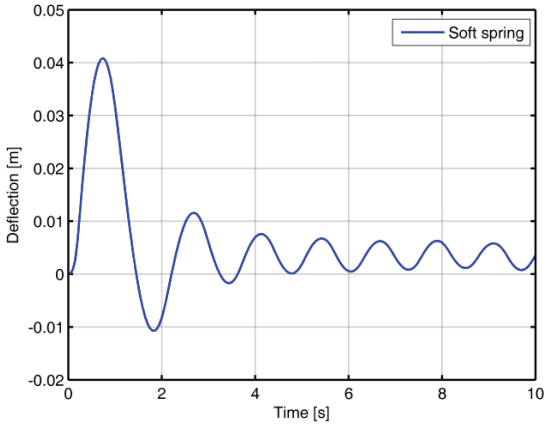

Figure 4b Deflection of the free end of the column under 1 kN external force, when the rotational spring at the column base has soft characteristics (Test 2).

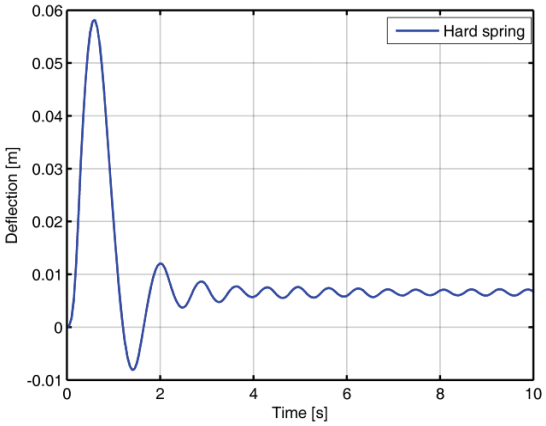

Figure 5a Deflection of the free end of the column under 2 kN external force when the rotational spring at the column base has hard characteristics (Test 3).

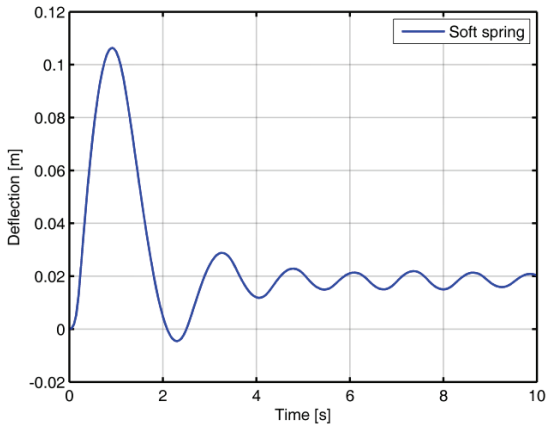

Figure 5b Deflection of the free end of the column under 2 kN external force when the rotational spring at the column base has soft characteristics (Test 4).

In the case of Tests 3 and 4 the external force is $F = 2$ kN acting under unchanged conditions compared to Test 1 and 2. The deflections of the hard and soft rotational springs are plotted in Fig. 5a and in Fig. 5b.

Although in the case of Tests 3 and 4 the amplitude of the acting external force is twice as high as in the case of Tests 1 and 2, the maximum value of the deflection at the free end of the column x_{max} in the two cases is more than twice, as it is shown in Tab. 1. At the same time it can be observed that the higher amplitude of external force requires longer time to reach the maximum deflection. At 1 kN external force the hard rotational spring reaches its maximum amplitude at 0,5 s in the case of Test 1, while in the case of Test 3 the maximum amplitude is reached in 0,6 s. Similar timing can be observed for the soft rotational spring.

Although the non-linear part of the rotational springs are modeled with hysteresis, the variation of the amplitude of the acting force does not have an effect on the cycling time of the hard and soft rotational springs.

It can be seen in Fig. 1 that in this investigated problem there is only an impulse force at the beginning of the simulation and there is no external force in the steady state. In spite of this there is an oscillating deflection and this deflection of the column is alternating around a non-zero constant value (x_0) according to the column mass m. Further investigation proves that the higher mass value results in higher value for the constant deflection (x_0), as it is shown in Tab. 2. In Tab. 2 tests 4-6 are compared in terms of parameters and results. For all tests in Tab. 2 the characteristic of the rotational spring is soft and the external force is 2 kN , see Fig. 6a and 6b.

By increasing the mass the maximum deflection of the column also increases. With the variation of the mass at the free end of the column, the cycling time (T_{osc}) changes as well, as this is shown in Tab. 2.

Table 2 Parameters and results of the numerical experiments Test 4 ÷ 6

Test	Mass / kg	T_{osc} / s	x_{max} / m	x_0 / m
4	10^3	1,25	0,1063	0,0185
5	2×10^3	1,85	0,0753	0,0219
6	3×10^3	2,50	0,0644	0,0288

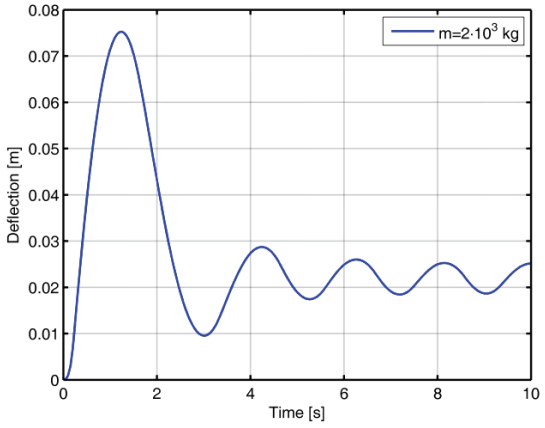

Figure 6a Deflection of the free end of the column when the mass is 2×10^3 kg at the free end and the rotational spring at the column base has soft characteristics (Test 5).

Next the effect of the time interval of the impulse force is studied for the rotational spring with medium hysteresis characteristics (Fig. 3b). For this study the mass at the free end of the column is 10^3 kg, the amplitude of the acting external force is 1 kN while the time interval of the acting force is varying as $\Delta t = 0{,}2$ s and $\Delta t = 0{,}4$ s . The results of the numerical simulation can be seen in Fig. 7a and Fig. 7b.

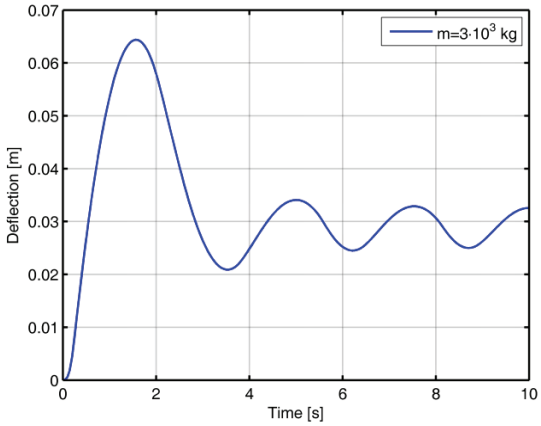

Figure 6b Deflection of the free end of the column when the mass is 3×10^3 kg at the free end and the rotational spring at the column base has soft characteristics (Test 6).

Table 3 Parameters and results of the numerical experiments Test 7 ÷ 8

Test	Δt / s	Spring	t_{max} / s	x_{max} / m	x_0 / m
7	0,2	medium	0,60	0,0307	0,0022
8	0,4	medium	0,85	0,0622	0,0060

From Fig. 7a and 7b and Tab. 3 it can be seen that the shorter force impulse results in lower deflection amplitude within shorter time under the same conditions. In the steady state the cycling time does not change, its value is around $T_{osc} = 1$ s . The constant component of the deflection for the force impulse acting for $\Delta t = 0{,}2$ s time interval is $x_0(0{,}2\text{ s}) = 0{,}0022$ m , for the force impulse acting for $\Delta t = 0{,}4$ s time interval the constant component of the deflection increases to $x_0(0{,}4\text{ s}) = 0{,}0060$ m .

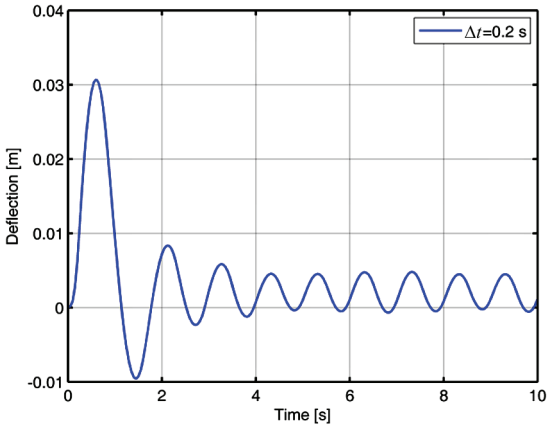

Figure 7a Deflection of the free end of the column when the impulse force is acting for 0,2 s and the rotational spring at the column base has medium characteristics (Test 7).

Finally the effect of the system-damping coefficient is investigated. In Fig. 8a the system-damping coefficient is zero $\alpha = 0\,\%$ with 10^3 kg mass and 1 kN external force

acting for $\Delta t = 0{,}2\,\mathrm{s}$ time interval, while the system-damping coefficient is $\alpha = 30\,\%$ under unchanged conditions in Fig. 8b.

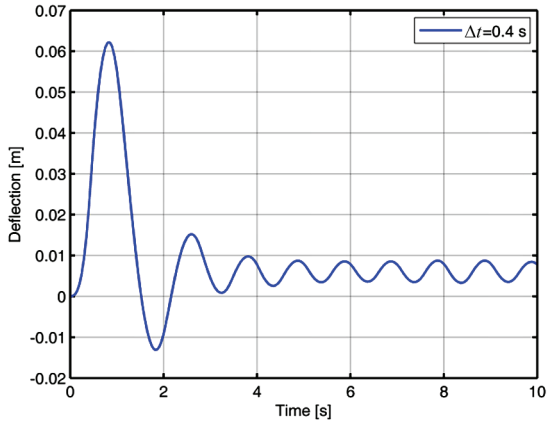

Figure 7b Deflection of the free end of the column when the impulse force is acting for 0,4 s and the rotational spring at the column base has medium characteristics (Test 8).

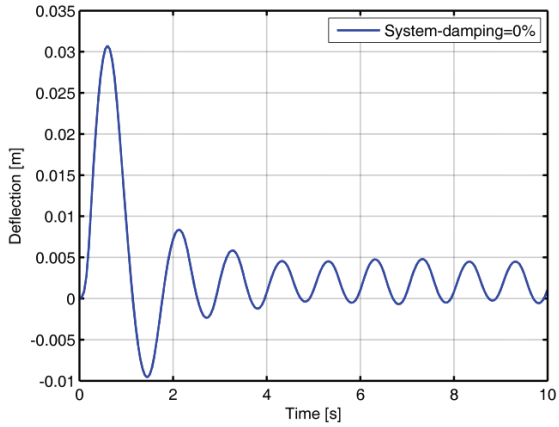

Figure 8a Deflection of the free end of the column when the system damping coefficient is 0 % and the rotational spring at the column base has medium characteristics (Test 9).

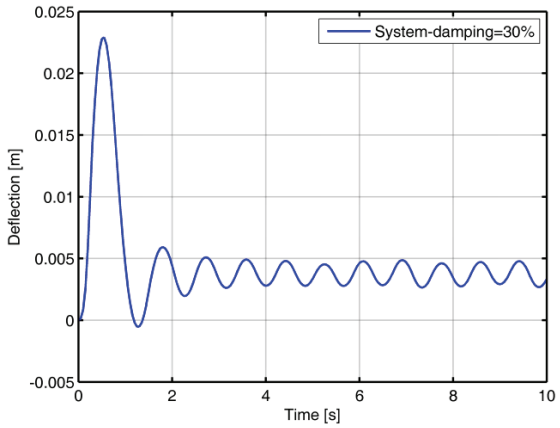

Figure 8b Deflection of the free end of the column when the system damping coefficient is 30 % and the rotational spring at the column base has medium characteristics (Test 10).

From the figures it can be seen that the system-damping coefficient has an influence on the transient period of the motion, however its effect is not too high on the steady state case. In the case of $\alpha = 0$ % the maximum amplitude of the deflection is $x_{max} = 0{,}0307$ m and in the case of $\alpha = 30$ % the maximum amplitude of the deflection is $x_{max} = 0{,}0229$ m. According to the system-damping effect the time to reach the maximum deflection becomes shorter, $t_{max}(\alpha = 0) = 0{,}6$ s, $t_{max}(\alpha = 30\,\%) = 0{,}55$ s. As an effect of the system-damping the vibration time is shorter, $T_{osc}(\alpha = 0\,\%) = 1$ s, $T_{osc}(\alpha = 30\,\%) = 0{,}8$ s. In the steady state the constant component of the deflection under the same conditions without system-damping is $x_0(\alpha = 0\,\%) = 0{,}0020$ m, while in the case of 30 % system-damping the constant component of the deflection is $x_0(\alpha = 30\,\%) = 0{,}0037$ m, it means that according to the system-damping effect the rotational spring has less plastic properties. In the case of 30 % system-damping the vibration amplitude is $x_{osc}(\alpha = 30\,\%) = 0{,}001$ m, while without system-damping this vibration amplitude is $x_{osc}(\alpha = 0\,\%) = 0{,}0025$ m.

5 Conclusions

In this paper a steel column has a semi-rigid boundary condition and a free end. An impulse force is acting on the free end of it. The mass of the column and some additional mass are concentrated at the free end of the column. The semi-rigid boundary condition is represented with a rotational spring of hysteretic properties, simulated by the Preisach hysteresis model. The response of the column has been determined with the solution of the non-linear motion equation, where the fix-point technique is implemented in the time marching iteration. Neglecting the system-damping effect the influence of the hard, medium and soft rotational spring on the deflection has been discussed. The effect of the change of the amplitude and the change of the time interval of the acting force impulse on the deflection has also been investigated. With the variation of the concentrated mass at the free end of the column, the maximum amplitude and the constant component in the oscillating deflection change as well as the vibration time. The considered 30 % system-damping value controls the transient response, however it has small influence on the steady state.

6 References

[1] Díaz, C.; Martí, P.; Victoria, M.; Querin, O. M. Review on the modeling of joint behavior in steel frames. // Journal of Constructional Steel Research, 67, (2011), pp. 741-758.

[2] Vandenbroucke, A.; Laurent, H.; Aït Hocine, N.; Rio, G. A hyperelasto-visco-hysteresis model for an elastometric behavior: Experimental and numerical investigations. // Computational Materials Science, 48, (2010), pp. 495-503.

[3] Kwofie, S. Description of cyclic hysteresis behavior based on one-parameter model. // Materials and Engineering, A357, (2003), pp. 86-93.

[4] Ramberg, W.; Osgood, W. R. Description of stress-strain curves by their parameters, Technical Note, No. 902, National Advisory Committee for Aeronautics, Washington DC, 1943.

[5] Mostaghel, N.; Byrd, R. A. Inversion of Ramberg-Osgood equation and description of hysteresis loop. // Int. J. of Non-Linear Mechanics, 37, (2002), pp. 1319-1335.

[6] Ni, Y. Q.; Wand, J. Y.; Ko, J. M. Advanced method for modeling hyteretic behavior of semi-rigid joints, in S. L. Chan, J. G. Teng (Eds.) Advances in Steel Structures, Elsevier, (1999), pp. 331-338.

[7] Ikhouane, F.; Rodellar, J. Systems with Hysteresis, Analysis, Identification and Control using the Bouc–Wen Model, Wiley, 2007.
[8] Ivanyi, A. Hysteresis models in electromagnetic computation, Akadémiai Kiadó, Budapest, 1997.
[9] Kuczmann, M.; Ivanyi, A. The finite element method in magnetics, Akademiai Kiado, Budapest, 2008.
[10] Krejci, P. Forced periodic vibrations of an elastic system with elasto-plastic damping. // Application of Mathematics, 33, (1988), pp. 145–153.
[11] Zienkiewicz, O. C.; Taylor, R. L. The Finite Element Method, Vol. 1, Fifth Edition, Butterworth & Heinemann, Oxford, 2000.
[12] Nagyová, M.; Psotný, M.; Ravinger, J. Stability and Friction. // Pollack Periodica, An Int. J. for Eng. and Information Sciences, 5, 3(2010), pp. 63-70.
[13] Györgyi, J. Dynamical systems, (in Hungarian), Budapest University of Technology and Economics, Budapest, 2003.
[14] Bottachio, O.; Chiampi, M.; Ragusa, C. Transient analysis of hysteretic field problems using fixed point technique. // IEEE Trans. on Magn, 34, (2003), pp. 1179-1182.
[15] M. Kuczmann, Vector Preisach hysteresis modeling, measurement, identification and application. // Physica B, Condensed Matter, 406, (2011), pp. 1403-1409.

Authors' addresses

Péter Iványi, PhD
Pollack Mihály Faculty of Engineering and Information Technology, University of Pécs
Pécs, Boszorkány u 2, 7624, Hungary
E-mail: peteri@morpheus.pte.hu